

# A stand-alone fiber-coupled single-photon source

Alexander Schlehahn<sup>1</sup>, Sarah Fischbach<sup>1</sup>, Ronny Schmidt<sup>1</sup>, Arseny Kaganskiy<sup>1</sup>, André Strittmatter<sup>1,2</sup>, Sven Rodt<sup>1</sup>, Tobias Heindel<sup>1,\*</sup>, and Stephan Reitzenstein<sup>1</sup>

<sup>1</sup>Institut für Festkörperphysik, Technische Universität Berlin, 10623 Berlin, Germany

<sup>2</sup>Present address: Abteilung für Halbleiterepitaxie, Otto-von-Guericke Universität, 39106 Magdeburg, Germany

\*tobias.heindel@tu-berlin.de

## ABSTRACT

In this work, we present a stand-alone and fiber-coupled quantum-light source. The plug-and-play device is based on an optically driven quantum dot delivering single photons via an optical fiber. The quantum dot is deterministically integrated in a monolithic microlens which is precisely coupled to the core of an optical fiber via active optical alignment and epoxide adhesive bonding. The rigidly coupled fiber-emitter assembly is integrated in a compact Stirling cryocooler with a base temperature of 35 K. We benchmark our practical quantum device via photon auto-correlation measurements revealing  $g^{(2)}(0) = 0.10^{+0.16}_{-0.10}$  under continuous-wave excitation and we demonstrate triggered non-classical light at a repetition rate of 80 MHz. The long-term stability of our quantum light source is evaluated by endurance tests showing that the fiber-coupled quantum dot emission is stable within  $\pm 3\%$  over several successive cool-down/warm-up cycles. Additionally, non-classical photon emission is demonstrated for a user-intervention-free 100-hour test run, showing stable single-photon count rates with a standard deviation of  $\pm 14\%$ .

## Introduction

Solid-state based quantum-light sources are elementary building blocks for future photonic quantum networks<sup>1</sup>, quantum information processing<sup>2</sup> and quantum metrology<sup>3</sup>. To date, the performance of non-classical light sources has reached such a high level, that the development of user-friendly devices for applications can be pursued. In particular, single-photon sources (SPSs) based on semiconductor quantum dots (QDs) show close to ideal properties in terms of the quantum nature of emission<sup>1</sup>, and sophisticated excitation schemes including strict resonant excitation enabled proof-of-principle demonstrations of photonic cluster-state generation<sup>4</sup> and boson sampling<sup>5,6</sup> in laboratory environments. Furthermore, field experiments using QD-based SPSs have been employed for proof-of-principle quantum key distribution experiments<sup>7</sup>, but still suffered from complex and bulky closed-cycle pulse-tube coolers and complex light extraction via free-space optics. Against this background, it is clear that fiber-coupling and robust packaging of practical quantum-light emitting devices is highly desirable for taking steps beyond proof-of-principle experiments. First steps in this direction utilized fiber-coupled QD-SPSs requiring fiber-bundles containing about 600 individual fiber cores to spatially post-select single emitter in a non-deterministic sample layout<sup>8</sup>. More recently, direct fiber-coupling of nitrogen-vacancies in nano-diamonds<sup>9</sup> and single QDs embedded in nanowires<sup>10</sup> were realized using complicated pick-and-place techniques, which are based on micromanipulators in a scanning electron microscope (SEM).

In this work, we report on a stand-alone and user-friendly quantum light source based on a fiber-coupled QD integrated within a compact Stirling cryocooler. The QD is deterministically embedded within a monolithic microlens via in-situ electron-beam lithography and precisely coupled to an optical fiber by employing an optical alignment-process and epoxide adhesive bonding at room-temperature. This concept allows for a high degree of control and reproducibility for the fabrication of stand-alone SPSs with pre-defined emission properties - features which are a key requirements for the upscaling of fiber-coupled quantum networks. To benchmark our source, we conduct photon auto-correlation measurements under continuous wave and pulsed optical excitation. Additionally, we demonstrate a high stability of the fiber-coupled single-photon emission over several cool-down/warm-up cycles as well as user-intervention-free long-term test runs, demonstrating the capability of our single-photon unit for autonomous operation in future photonic quantum networks.

## Results

### Fiber-coupling of deterministic QD microlenses

The stand-alone SPS is based on a wafer grown by metal-organic chemical vapour deposition on GaAs-(001) substrate. After a 300 nm thick GaAs buffer layer, a distributed Bragg reflector consisting of 23 pairs of  $\lambda/4$ -thick  $\text{Al}_{0.9}\text{Ga}_{0.1}\text{As}/\text{GaAs}$  is deposited. Next, 65 nm of GaAs, a single layer of self-organized InAs QDs and a 420 nm thick GaAs capping layer are grown. For the optical alignment procedure of the fiber core to a QD-microstructure, a 80 nm-thick gold mask containing  $10\mu\text{m} \times 10\mu\text{m}$

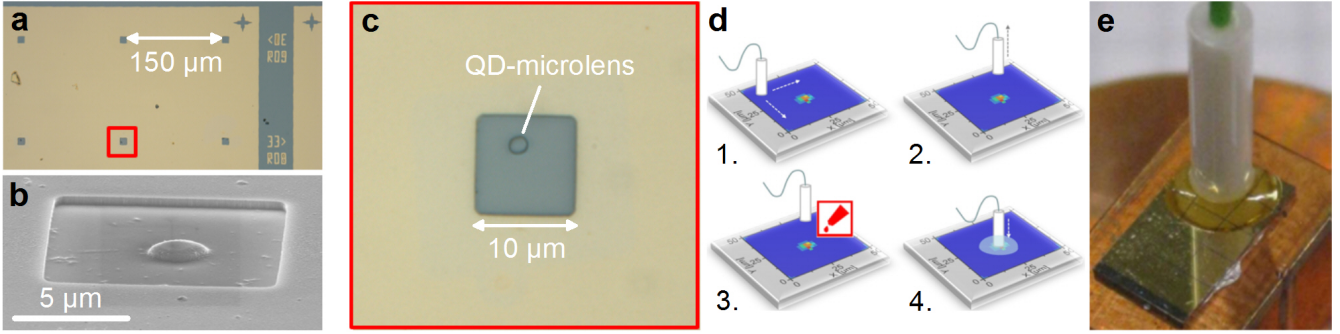


**Figure 1.** Fabrication of fiber-coupled QD microlenses. (a) Microscope image of the sample surface before fiber-coupling. A gold-mask contains arrays of apertures with a pitch of  $150\ \mu\text{m}$ . Each target aperture contains a single deterministically fabricated QD-microlens. Marker structures allow for unambiguous identification of target apertures and microlenses. (b) SEM image of a deterministic single-QD microlens fabricated via 3D in-situ electron-beam lithography and reactive ion etching. (c) Microscope image of a single aperture (dimensions:  $10\ \mu\text{m} \times 10\ \mu\text{m}$ ) containing a microlens deterministically fabricated above a pre-selected QD. Suitable QD-microlenses are pre-characterized using standard micro-photoluminescence spectroscopy at 10 K. (d) Illustration of the room-temperature fiber-coupling process: 1. Fiber-scan across sample surface and monitoring of GaAs-bandgap emission within the gold apertures excited by 651 nm laser. Emission of the bandgap is only visible above apertures and markers. 2. Precise alignment of the fiber above a precharacterized target aperture and lifting of the fiber by about 5 mm. 3. Attaching a small drop of epoxide adhesive to the fiber-ferrule. 4. Lowering of the fiber to its previous position and monitoring of GaAs emission during hardening ( $\approx 2$  hours). (e) Photograph of a fiber-coupled QD sample after the process illustrated in (d) showing the fiber ferrule glued to the sample.

apertures with a pitch of  $150\ \mu\text{m}$  and corresponding markers (for unambiguous identification) is defined via optical (UV) lithography (cf. Figure 1 a). Subsequently, the sample is spin-coated with a 100 nm-thick layer of the electron-beam resist AR-P 6200 (CSAR 62)<sup>11</sup> and transferred to a low-temperature cathodoluminescence lithography (CLL) system. The latter consists of a SEM with integrated liquid-helium flow-cryostat and extensions for optical spectroscopy as well as electron-beam lithography<sup>12</sup>. Using the 3D in-situ electron beam lithography at 10 K<sup>13,14</sup>, we define single deterministic QD-microlenses in the gold apertures. Afterwards the sample is transferred out of the CLL system and the resist is developed. This leaves the cross-linked resist above target QDs acting as lens-shaped etch masks for the subsequent etch step using reactive-ion-enhanced plasma etching (etch depth: 420 nm). This directly transfers the lens-profile into the semiconductor material (i.e. GaAs). As a result of the described fabrication process, our sample is covered by a gold mask containing apertures with one deterministic QD-microlens (diameter:  $2.4\ \mu\text{m}$ ) each (cf. Figure 1 b and c), while all other (non-selected) QDs inside apertures were removed by the dry-etching process. Using micro-photoluminescence spectroscopy at 10 K, suitable QD-microlenses are selected according to their PL intensity.

For the precise coupling of a photonic QD-microstructure to an optical fiber, we developed an alignment technique which combines deterministic in-situ QD-device fabrication with a robust optical coupling of the fiber core using epoxide adhesive bonding at ambient conditions (room temperature, no vacuum). In the developed process we scan a multi-mode fiber with  $50\ \mu\text{m}$  core-diameter embedded in a ceramic ferrule in short distance (see below) across the sample surface using a 3D closed-loop piezo-stage, as illustrated in Figure 1 d. The light of a CW laser ( $\lambda = 671\ \text{nm}$ ) coupled into the fiber is reflected at the gold mask. If the fiber core is located above an aperture, charge-carriers are generated inside the semiconductor material and the associated photoluminescence of the GaAs bandgap (around 870 nm at 300 K) can easily be detected using a spectrometer attached to the output of the scanning fiber. The pitch of  $150\ \mu\text{m}$  between apertures in combination with alignment markers allows us to precisely locate target apertures containing a single QD-microlens, which was pre-characterized via  $\mu\text{PL}$ . The height of the scanning fiber is thereby adjusted by observing the luminescence of the GaAs-bandgap in the following way: If the fiber ferrule is gently pressed to the sample surface, the resulting strain leads to a slight spectral shift of the bandgap emission. Moving the fiber back to the position of the unstrained GaAs-bandgap defines the point of physical contact.

After locating the target aperture, the fiber is lifted by about 5 mm normal to the sample surface. At this point, a small drop of epoxide adhesive is attached to the fiber-ferrule and the fiber is lowered to its previous position. The final position has to be reached within the epoxide pot life of about 5 minutes. Until the hardening process is completed ( $\approx 2$  hours), the emission of the GaAs bandgap is monitored continuously to detect a possible misalignment between fiber-core and aperture. To test the accuracy of our fiber-coupling procedure, we repeated the process described above for fiber-core diameters of  $25\ \mu\text{m}$  and  $9\ \mu\text{m}$ . In all cases we were able to precisely locate the positions of the apertures, suggesting an alignment accuracy better than  $9\ \mu\text{m}$ .

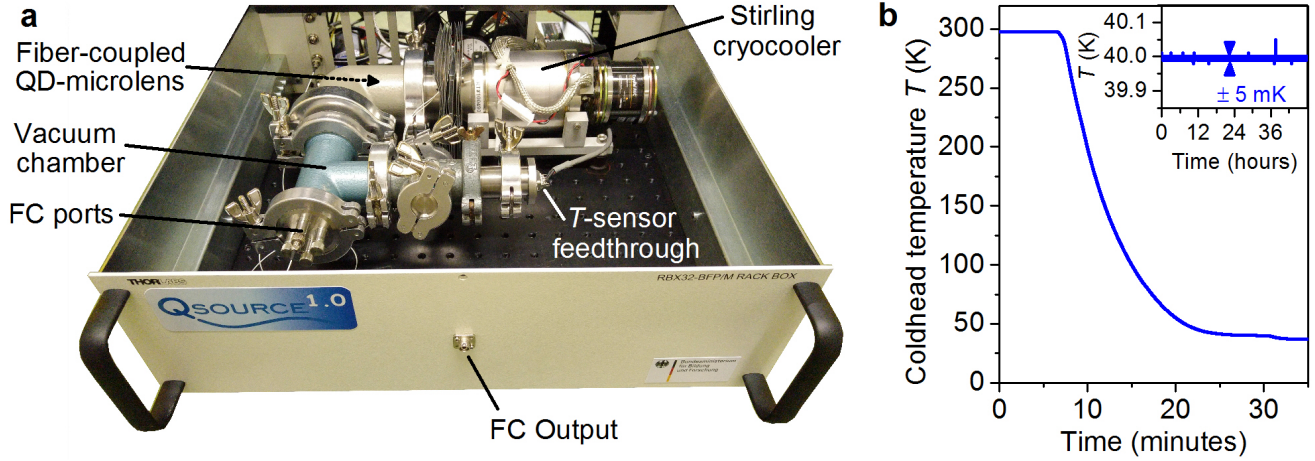


**Figure 2.** The stand-alone single-photon source 'QSource'. (a) QSource module comprising the Stirling cryocooler with attached customized vacuum chamber. The fiber-coupled (FC) QD-microlens (cf. Figure 1) is mounted to the cryocooler's coldhead inside the vacuum chamber. (c) Coldhead temperature of the Stirling cryocooler measured during cool-down. Inset: Coldhead temperature over a measurement period of 48 hours, revealing high temperature stability of the cryocooler.

The presented approach for fiber-coupling has several advantages: Firstly, the complete alignment and curing process is performed under ambient conditions, and neither requires cryogenic temperatures for QD identification nor heating or UV illumination during hardening of the adhesive. This makes our process robust, easy to use and economic, and still enables a high accuracy of the alignment allowing for single-mode fiber-coupling. Secondly, the fiber is embedded in a ceramic ferrule which increases the bond area and hinders the fiber from being torn off by torsional forces appearing when handling the fiber-coupled device. Additionally, we use a commercially available and quickly reactive epoxide for curing, which is developed for fiber connector preparation and is thus index matched to optical fibers. The index matching between fiber-core and adhesive further reduces reflection losses at the interface which can further enhance the extraction efficiency. Moreover, our approach can easily be adopted for other solid-state based SPSs, such as micropillar cavities<sup>15</sup> and bullseye resonators<sup>16</sup>, as well as for SPSs emitting at telecom wavelengths.

### Stand-alone single-photon unit

When operated at cryogenic temperatures, the InAs/GaAs material system used for the QD-SPS in our work offers superior quantum optical properties<sup>17,18</sup> if compared to quantum emitters operated at room temperature<sup>19–23</sup>. Thus, a crucial aspect for the development of high-quality and user-friendly SPSs is the cooling of the quantum emitter to cryogenic temperatures. To date, liquid helium supplied in large storage dewars in combination with flow-cryostats is still the most common cooling technique in research laboratories. However, aiming at the autonomous operation of a quantum light source at remote places without laboratory infrastructure requires more practical cryocoolers. In recent years the use of closed-cycle pulse-tube coolers for experiments in quantum optics have become more popular, due to improvements in vibration damping<sup>7</sup>. Although such systems do not require a permanent liquid helium supply, they still depend on high-power voltage supplies and bulky compressors.

In our work, we employ a compact and economic Stirling cryocooler<sup>24</sup> to build a stand-alone fiber-coupled SPS (see Figure 2 a), called 'QSource' in the following. The Stirling cryocooler only requires a standard supply voltage (220 V), can be operated with minimal space requirements and recently proved to be suitable for quantum-optical free-space experiments at base temperatures down to 30 K<sup>25</sup>. The Stirling cryocooler (Model: Cryotel-GT from Sunpower) used in our QSource comprises a single piston moving along the same axis as the movable regenerator which allows for compact dimensions of 27.6 cm  $\times$  8.3 cm  $\times$  8.3 cm. The cryocooler is additionally equipped with an active counter balancer, efficiently reducing vibration export from the moving piston to the coldhead. The fiber-coupled SPS described in the previous section is mounted directly to the cryocooler's coldhead. A custom made vacuum chamber attached to the Stirling cryocooler encloses the coldhead and contains ports for up to four optical fibers and the electrical-feedthroughs for the temperature sensor integrated into the coldhead.

Due to the compact dimensions of the Stirling cryocooler, the complete single-photon unit including the vacuum chamber with all necessary feedthroughs fits easily within a standard 19" rack-insert as depicted in Figure 2 b). For an autonomous operation of our QSource, the single-photon unit is housed in a small mobile rack (90 cm height) containing a diode laser ( $\lambda = 651$  nm or 855 nm, continuous wave (CW) or pulsed mode) coupled to the single-photon unit via a 90:10 fiber beamsplitter,

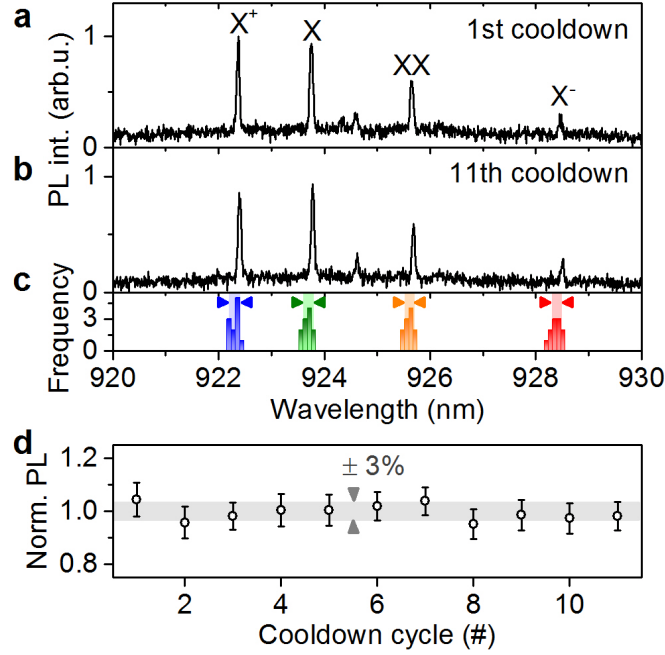


**Figure 3.** Durability test of the fiber-connection. (a) Spectrum of a fiber-coupled QD-microlens (SPS1) operated in our QSource at  $T = 40$  K. Emission of the exciton (X), the biexciton (XX), and singly charged trion states ( $X^+$  and  $X^-$ ) is identified. (b) Spectrum of SPS1 after 11 cool-down/warm-up cycles (40 K  $\leftrightarrow$  290 K). (c) Frequency count histogram of the center wavelength of the four QD states extracted from the spectra of 11 consecutive cool-down/warm-up cycles. (d) Integrated and normalized intensity of the fiber-coupled QD-emission for cooldown cycle 1 to 11.

the electronics for controlling the Stirling cryocooler and a personal computer (PC) with display, keyboard and mouse. Via the PC the user is able to control all parameters relevant for operation of the QSource, including temperature control and monitoring. Additionally, it optionally allows for photon-autocorrelation measurements using a fiber-based Hanbury-Brown and Twiss (HBT) setup equipped with two Silicon-based single-photon counting modules (SPCMs) and the corresponding electronics for time-correlated single-photon counting (TCSPC). The temperature at the coldhead during a cool-down of the Stirling-cryocooler is depicted in Figure 2 c. After only 30 minutes the sample reaches a temperature of 40 K. The inset shows a measurement of the coldhead temperature over a period of 48 hours, revealing a mean base temperature of 39.995 K at a temperature stability of  $\pm 6$  mK being competitive with state-of-the-art Helium-flow cryostats and about one order of magnitude improvement compared to our previous work Ref.<sup>25</sup>.

### Durability of fiber-coupling

The spectral properties and the durability of our fiber-coupled SPS are tested using a spectrometer with a 1200-lines optical grating and an attached liquid-Nitrogen-cooled charge-coupled device camera (system's spectral resolution:  $25 \mu\text{eV}$ ). Figure 3 a presents the spectrum of a fiber-coupled QD-microlens, named SPS1 from now on, operated in our QSource at 40 K (integration time: 1 s). Emission of different excitonic states stemming from the same QD is clearly observed, where the charge-neutral exciton (X), the biexciton (XX) and the singly charged trion states ( $X^+$  and  $X^-$ ) were identified via polarization- and excitation-power-resolved measurements (not shown).

To evaluate the durability of the glued connection between optical fiber and QD sample, we repeatedly warmed up and cooled down the sample and monitored the emission of SPS1 in the following way using an automated routine. Starting from room temperature (290 K), the Stirling cryocooler is turned on in power-controlled mode (110 W). After reaching the base temperature, the system holds this temperature for 30 minutes to reach thermal equilibrium. Then the coldhead temperature is stabilized at 40 K using a proportional-integral-derivative (PID) -controlled operation mode for 10 minutes and a spectrum is recorded before the Stirling cryocooler is turned off. The next cooling cycle starts automatically after the coldhead reached room temperature again (about 6 hours). Figure 3 b displays the spectrum of SPS1 after the 11th cooldown cycle. The emission properties of the QD in terms of the spectral finger print and the emission intensities of the corresponding excitonic states remain almost unchanged, indicating a high durability of the glued connection between fiber and sample. Quantitatively extracting the emission energies of the four QD states for each spectrum from cooldown cycle 1 to 11 by fitting yields standard deviations for



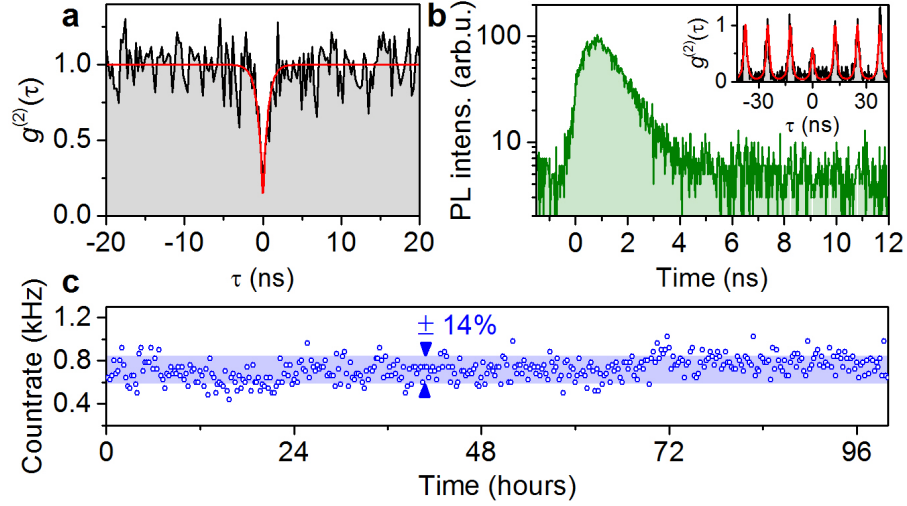


**Figure 4.** Single-photon generation using the QSource. (a) Measurement of the second-order photon-autocorrelation  $g^{(2)}(\tau)$  of the X-emission of SPS1 (cf. Figure 3) operated in the Stirling cryocooler demonstrating single-photon emission with  $g^{(2)}(0) = 0.10^{+0.16}_{-0.10}$ . (b) Time-resolved measurement of the fiber-coupled emission of SPS2 under pulsed excitation at 80 MHz. Inset:  $g^{(2)}(\tau)$ -histogram recorded for SPS2, revealing triggered non-classical light emission. (c) Single-photon countrates of SPS2 recorded via single-photon counting modules during a user-intervention-free test run over a period of 100 hours.

the spectral shifts of  $\delta E_{X+} = \pm 86$  pm,  $\delta E_X = \pm 85$  pm,  $\delta E_{XX} = \pm 84$  pm and  $\delta E_{X-} = \pm 98$  pm. The corresponding frequency histogram of the fitting results is shown in Figure 3 c. The small deviation in emission energy over many cooldown cycles is attributed to slightly varying electric fields in the vicinity of the QD due to charge fluctuations and the resulting quantum confined Stark effect<sup>26</sup>. Interestingly, a careful analysis of the data reveals that the relative spectral positions of all four emission lines with respect to the X-state remains constant within a standard deviation of  $\pm 4$  to  $\pm 7$  pm, more than one order magnitude less than the absolute spectral shift. Thus we conclude, that the binding energies of the respective QD-states remain almost constant over the entire 11 cooldown cycles, implying that the strain inside the QD sample is not changing over time, which confirms the high stability of our fiber-coupling scheme. Additionally, we evaluate the change in brightness of SPS1 during the durability test. Figure 3 d depicts the normalized integrated intensity of the QD emission, obtained by summing up the integrated intensities of the excitonic complexes for each spectrum. We observe, that the emission of SPS1 is stable within a  $\pm 3\%$  standard deviation, certifying an excellent durability of the glued fiber connection used in our QSource.

### Turn-key single-photon generation

To evaluate the performance of our stand-alone single-photon source in terms of its single-photon purity, we performed measurements of the second-order photon-autocorrelation  $g^{(2)}(\tau)$  during operation of the Stirling cryocooler at cryogenic temperature ( $T = 40$  K). For this purpose, the fiber-output of the QSource is spectrally filtered (bandwidth: 0.1 nm) via the external spectrometer transmitting the emission of the exciton state X. Right after the spectrometer, the X emission is coupled to the fiber-based HBT setup for coincidence measurements. Figure 4 a presents the histogram of  $g^{(2)}(\tau)$  (time-bin width: 275 ps) under CW excitation at 651 nm. The pronounced antibunching at zero time delay ( $\tau = 0$ ) signifies the non-classicality of the emitted light. Indeed, fitting the experimental data by accounting for the timing resolution (350 ps) of the HBT setup reveals  $g^{(2)}(0) = 0.10^{+0.16}_{-0.10}$  unambiguously demonstrating single-photon emission.

With respect to applications of single-photon sources in quantum information, triggered emission of single-photons is required. We therefore tested the QSource under pulsed-excitation at 855 nm with an excitation repetition rate of 80 MHz (pulse-width: 80 ps) using another single-photon source (SPS2) as quantum emitter. The time-resolved fiber-coupled emission of an excitonic state is displayed in Figure 4 b. The optical response of the QD-state shows a monoexponential decay with a lifetime of  $1.0 \pm 0.1$  ns. The corresponding  $g^{(2)}(\tau)$ -histogram under pulsed excitation is depicted in the inset of Figure 4 b. The clearly separated coincidence peaks combined with the significantly suppressed peak at zero delay, prove triggered emission of non-classical light. Fitting the experimental data with a model according to Ref.<sup>27</sup> yields antibunching with  $g^{(2)}(0) = 0.57 \pm 0.05$ . The non-ideal antibunching is limited by the uncorrelated background emission of the nearby wetting layer for this particular sample. Additionally, we evaluated the long-term stability of the single-photon flux at the output of our QSource. For this purpose, we recorded the single-photon count rates of the SPCMs over a period of 100 hours (see Figure 4 c). We observe a single-photon detection rate of 720 Hz (including 41 Hz dark counts) being stable within  $\pm 14\%$  over the entire

100-hour measurement period without any user intervention.

## Summary and outlook

In this work, we report on a user-friendly stand-alone SPS providing single-photon emission via an optical fiber. Within our single-photon unit, a QD is deterministically embedded in a monolithic microlens. The precise coupling of the QD-microlens to the optical fiber is achieved using a robust process based on active alignment and epoxide adhesive bonding at room-temperature, which allows for an accuracy better than  $9\text{ }\mu\text{m}$ . The fiber-coupled single-photon emitter is mounted to the coldhead of a compact plug-and-play Stirling cryocooler integrated in a 19" rack-insert. Our stand-alone device allows for autonomous operation over several days with high stability of the single-photon flux at the fiber output and antibunching values down to  $g^{(2)}(0) = 0.10^{+0.16}_{-0.10}$ . Moreover, we show triggered emission of non-classical light at 80 MHz excitation repetition rate. The high durability of the fiber-connection is proven in endurance tests, revealing stable integrated QD emission within  $\pm 3\%$  over more than 10 successive cooldown cycles. Additionally, a user-intervention-free 100-hour test run, yields stable single-photon countrates with a standard deviation of  $\pm 14\%$ , confirming the potential of our approach for applications in quantum information science.

By implementing straight forward extensions to our QSource, we anticipate greatly enhanced performance in terms of the achievable single-photon purity and flux. For instance, by combining our deterministic QD-microlenses with miniaturized laser-written multi-lens objectives<sup>28</sup>, the photon extraction efficiency from our device as well as the coupling efficiency to an optical fiber can be enhanced<sup>29</sup>. Moreover, a higher level of integration will reduce the total system losses. This can for instance be achieved by using electrically pumped quantum light sources by utilizing a recently developed contacting scheme for deterministic QD microlenses<sup>30</sup> or by employing compact interference band-pass filters instead of bulky external spectrometers<sup>31</sup>. Additionally, the accuracy of our fiber-coupling process also allows for the use of single-mode fibers, which is highly beneficial for applications in quantum optics. Finally, the next-generation QSource can easily be adapted to other operation wavelengths, opening up the route for the realization of turn-key stand-alone quantum light sources at telecommunication wavelengths for applications in fiber-based quantum key distribution and quantum repeater networks.

## References

1. Aharonovich, I., Englund, D. & Toth, M. Solid-state single-photon emitters. *Nat. Photonics* **10**, 631–641 (2016).
2. Kok, P. *et al.* Linear optical quantum computing with photonic qubits. *Rev. Mod. Phys.* **79**, 135–174 (2007).
3. Giovannetti, V., Lloyd, S. & Maccone, L. Quantum-enhanced measurements: Beating the standard quantum limit. *Sci.* **306**, 1330–1336 (2004).
4. Schwartz, I. *et al.* Deterministic generation of a cluster state of entangled photons. *Sci.* **354**, 434–437 (2016).
5. Wang, H. *et al.* Multi-photon boson-sampling machines beating early classical computers. *Prepr. at <https://arxiv.org/abs/1612.06956>* (2016).
6. Loredó, J. C. *et al.* Boson sampling with single-photon fock states from a bright solid-state source. *Phys. Rev. Lett.* **118**, 130503 (2017).
7. Rau, M. *et al.* Free space quantum key distribution over 500 meters using electrically driven quantum dot single-photon sources - a proof of principle experiment. *New J. Phys.* **16**, 043003 (2014).
8. Xu, X. *et al.* "plug and play" single-photon sources. *Appl. Phys. Lett.* **90**, 061103 (2007).
9. Schröder, T., Schell, A. W., Kewes, G., Aichele, T. & Benson, O. Fiber-integrated diamond-based single photon source. *Nano Lett.* **11**, 198–202 (2011).
10. Cadeddu, D. *et al.* A fiber-coupled quantum-dot on a photonic tip. *Appl. Phys. Lett.* **108**, 011112 (2016).
11. Kaganskiy, A., Heuser, T., Schmidt, R., Rodt, S. & Reitzenstein, S. CSAR 62 as negative-tone resist for high-contrast e-beam lithography at temperatures between 4k and room temperature. *J. Vac. Sci. & Technol. B, Nanotechnol. Microelectron. Materials, Process. Meas. Phenom.* **34**, 061603 (2016).
12. Gschrey, M. *et al.* Resolution and alignment accuracy of low-temperature in situ electron beam lithography for nanophotonic device fabrication. *J. Vac. Sci. & Technol. B* **33**, 021603 (2015).
13. Gschrey, M. *et al.* In situ electron-beam lithography of deterministic single-quantum-dot mesa-structures using low-temperature cathodoluminescence spectroscopy. *Appl. Phys. Lett.* **102**, 251113 (2013).
14. Gschrey, M. *et al.* Highly indistinguishable photons from deterministic quantum-dot microlenses utilizing three-dimensional in situ electron-beam lithography. *Nat Comms* **6**, 7662 (2015).

15. Heindel, T. *et al.* Electrically driven quantum dot-micropillar single photon source with 34% overall efficiency. *Appl. Phys. Lett.* **96**, 011107 (2010).
16. Ates, S., Sapienza, L., Davanco, M., Badolato, A. & Srinivasan, K. Bright single-photon emission from a quantum dot in a circular bragg grating microcavity. *Sel. Top. Quantum Electron. IEEE J.* **18**, 1711–1721 (2012).
17. Michler, P. *et al.* A quantum dot single-photon turnstile device. *Sci.* **290**, 2282–2285 (2000).
18. Ding, X. *et al.* On-demand single photons with high extraction efficiency and near-unity indistinguishability from a resonantly driven quantum dot in a micropillar. *Phys. Rev. Lett.* **116** (2016).
19. Michler, P. *et al.* Quantum correlation among photons from a single quantum dot at room temperature. *Nat.* **406**, 968–970 (2000).
20. Kurtsiefer, C., Mayer, S., Zarda, P. & Weinfurter, H. Stable solid-state source of single photons. *Phys. Rev. Lett.* **85**, 290–293 (2000).
21. Lounis, B. & Moerner, W. E. Single photons on demand from a single molecule at room temperature. *Nat.* **407**, 491–493 (2000).
22. Holmes, M. J., Choi, K., Kako, S., Arita, M. & Arakawa, Y. Room-temperature triggered single photon emission from a iii-nitride site-controlled nanowire quantum dot. *Nano Lett.* **0**, null (2014).
23. Deshpande, S., Frost, T., Hazari, A. & Bhattacharya, P. Electrically pumped single-photon emission at room temperature from a single ingan/gan quantum dot. *Appl. Phys. Lett.* **105**, 141109 (2014).
24. Veprik, A., Riabzev, S., Vilenchik, G. & Pundak, N. Ultra-low vibration split stirling linear cryogenic cooler with a dynamically counterbalanced pneumatically driven expander. *Cryog.* **45**, 117 – 122 (2005).
25. Schlehahn, A. *et al.* Operating single quantum emitters with a compact stirling cryocooler. *Rev. Sci. Instruments* **86**, 013113 (2015).
26. Empedocles, S. A. & Bawendi, M. G. Quantum-confined stark effect in, cdse nanocrystallite quantum dots. *Sci.* (1997).
27. Schlehahn, A. *et al.* An electrically driven cavity-enhanced source of indistinguishable photons with 61% overall efficiency. *APL Photonics* **1** (2016).
28. Gissibl, T., Thiele, S., Herkommer, A. & Giessen, H. Two-photon direct laser writing of ultracompact multi-lens objectives. *Nat. Photon* (2016).
29. Fischbach, S. *et al.* Single quantum dot with microlens and 3D printed microobjective as integrated bright single-photon source. *unpublished* (2017).
30. Schlehahn, A. *et al.* Generating single photons at gigahertz modulation-speed using electrically controlled quantum dot microlenses. *Appl. Phys. Lett.* **108**, 021104 (2016).
31. Heindel, T. *et al.* Quantum key distribution using quantum dot single-photon emitting diodes in the red and near infrared spectral range. *New J. Phys.* **14**, 083001 (2012).

## Acknowledgements

We acknowledge support from the German Federal Ministry of Education and Research (BMBF) via the VIP-project QSOURCE (Grant No. 03V0630), the German Research Foundation (DFG) via the SFB 787 'Semiconductor Nanophotonics: Materials, Models, Devices', the European Research Council under the European Union's Seventh Framework ERC Grant Agreement No. 615613, and the project EMPIR 14IND05 MIQC<sup>2</sup> (the EMPIR initiative is co-funded by the European Unions Horizon 2020 research and innovation programme and the EMPIR Participating States).

## Author contributions statement

A. Schlehahn and T.H. developed the stand-alone single-photon source, performed the spectroscopy and correlation experiments and analyzed the experimental data. S.F. performed the CL lithography and processed the samples together with R.S. under supervision of S. Rodt. A.K. and A. Strittmatter grew the samples. T.H. wrote the manuscript with input from all authors. S. Reitzenstein supervised the project.